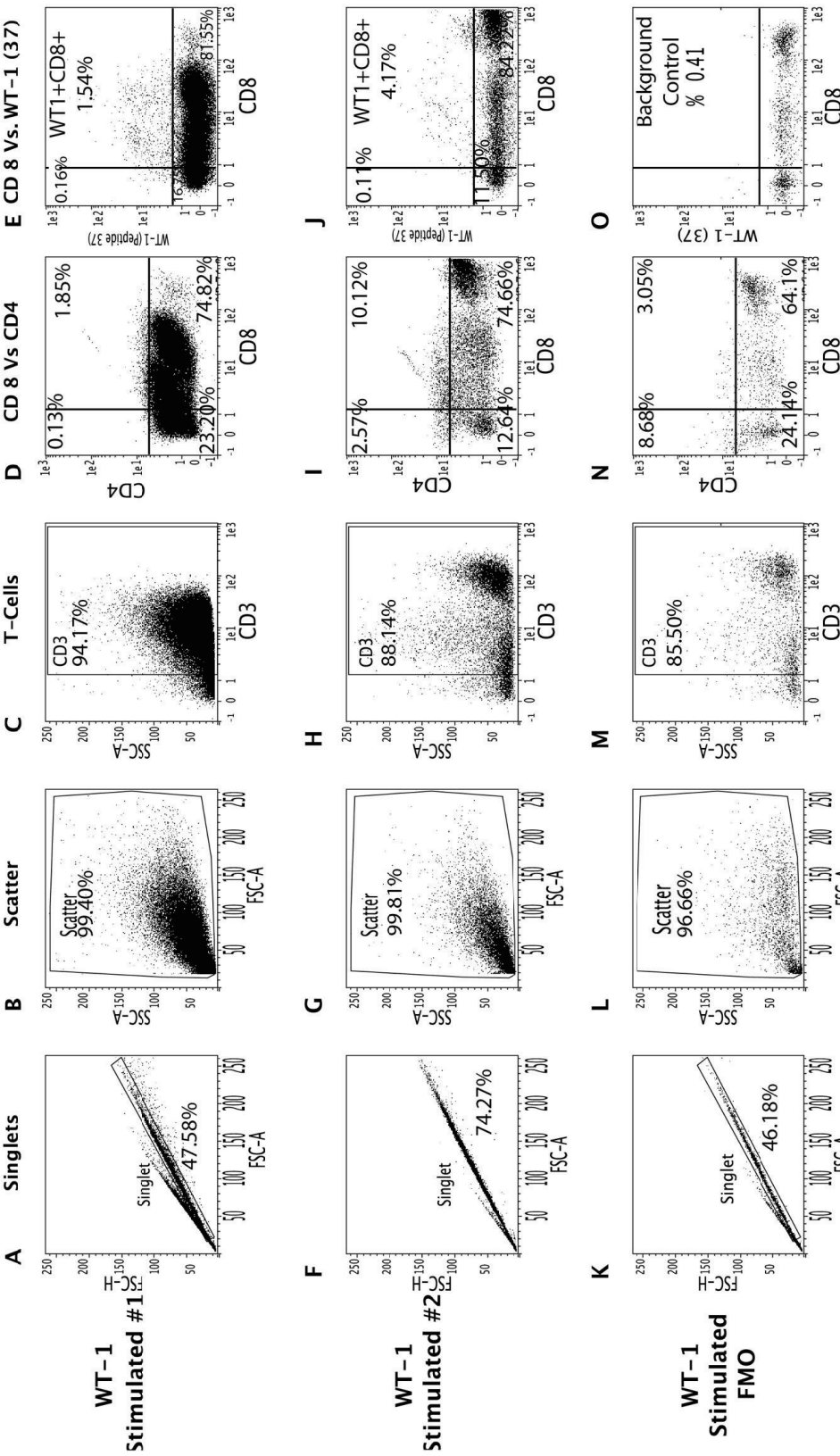
Figures 1A-1O
Stimulation of cytotoxic T cells specific for Wilm's Tumor 1 (WT-1) antigen



Figures 2A-2G
CD8+ Cytotoxic T cells with TCR specific for Wilm's Tumor (WT-1) antigen are functional

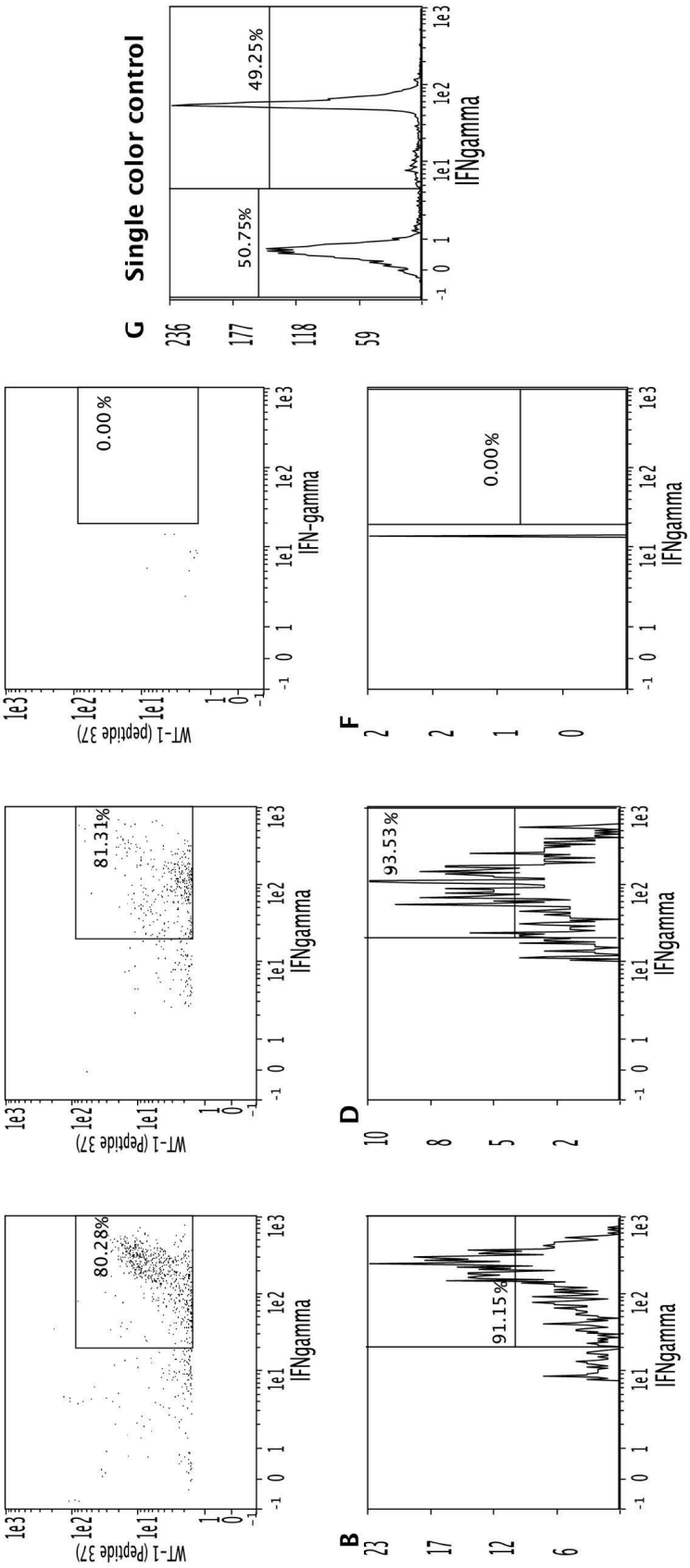


Figure 2H
LAG 3 inhibitor (IMP 321) increases the frequency of WT-1 specific T cells

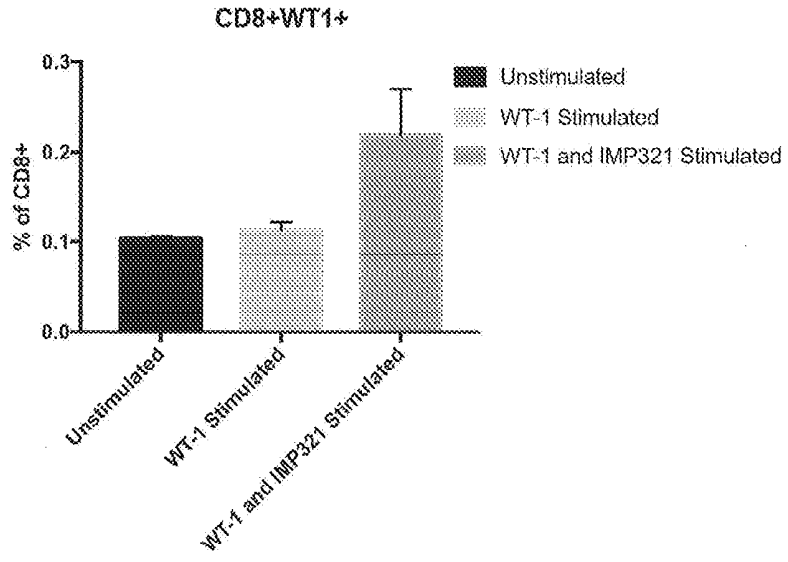


Figure 3
Production of iPSC from cancer specific (eg WT-1) TCR T cells

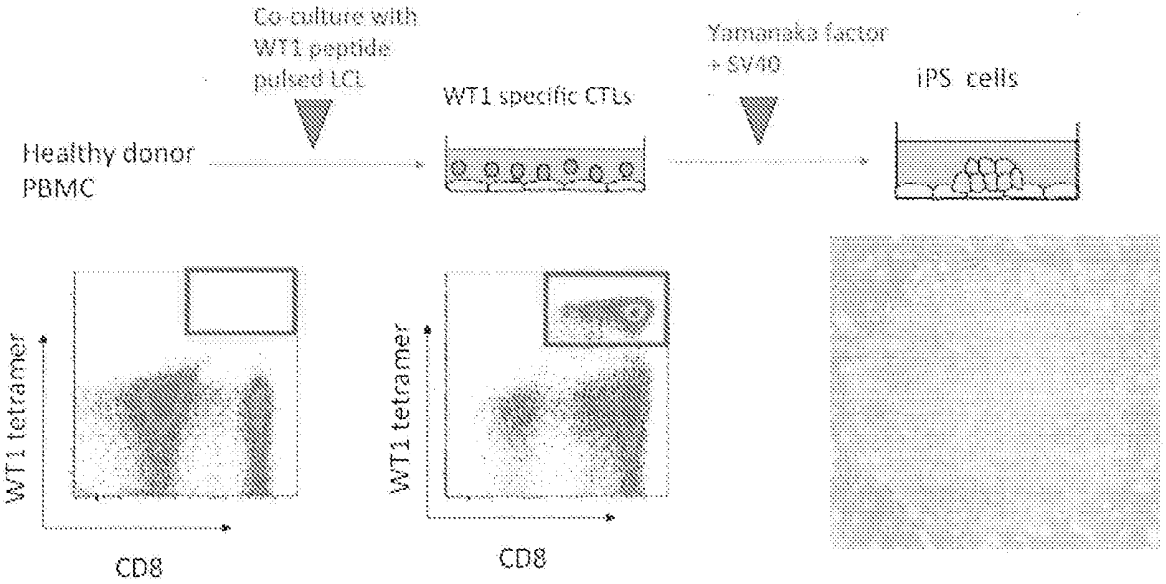


Figure 4
Differentiation of iPSC to hematopoietic T-cell precursors on OP9 feeder layers

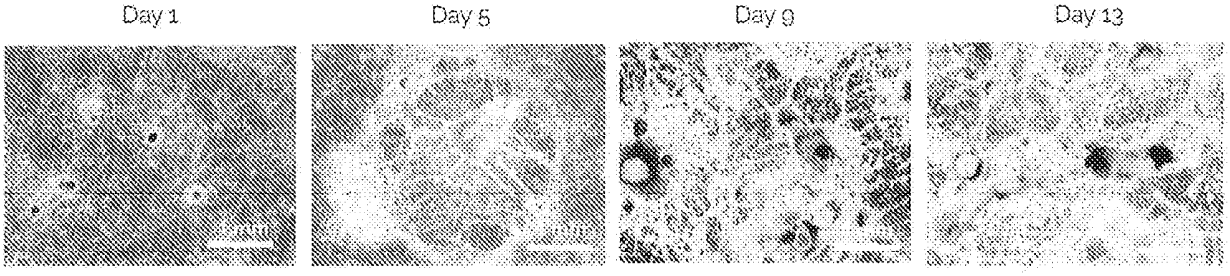


Figure 5
HSC-like cells are present after 13 days culture on OP9 cells

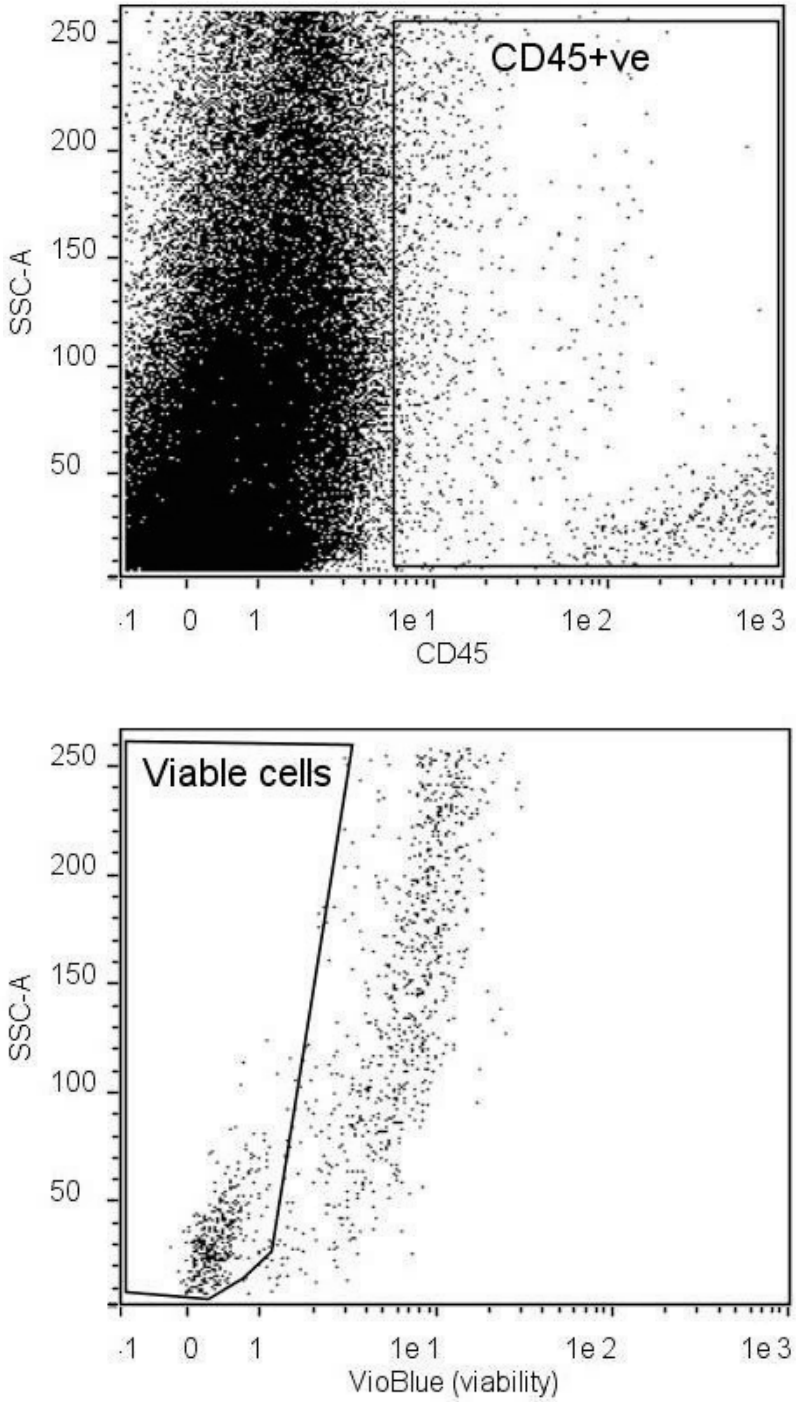
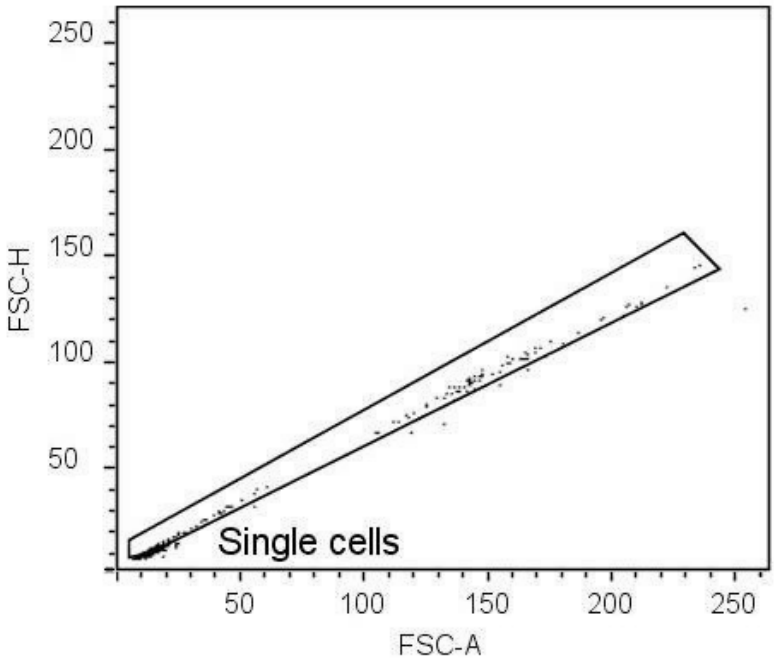


Figure 5 (Continued)



HSC profile: CD34+ CD43+

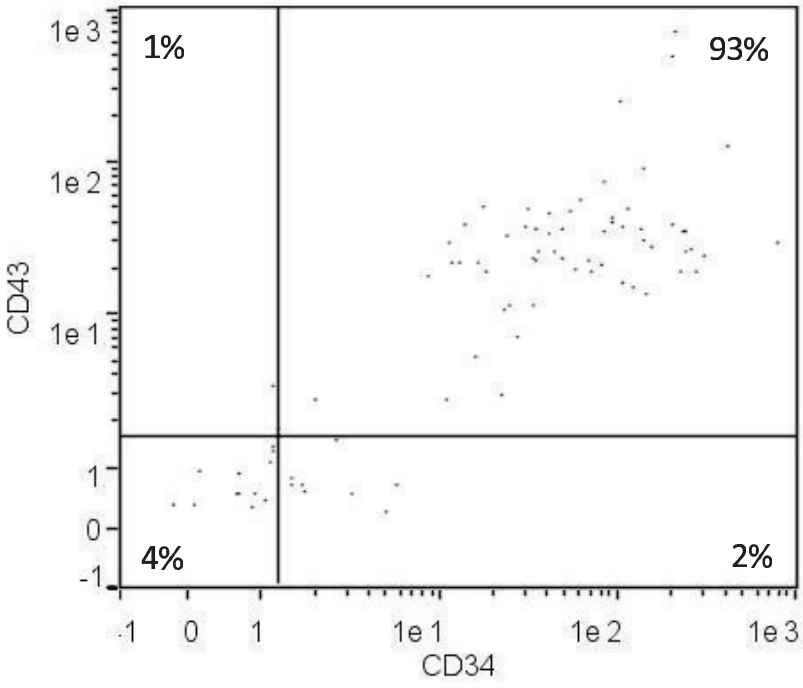


Figure 6
HSC are reduced after 9 days culture on OPDL-1 cells

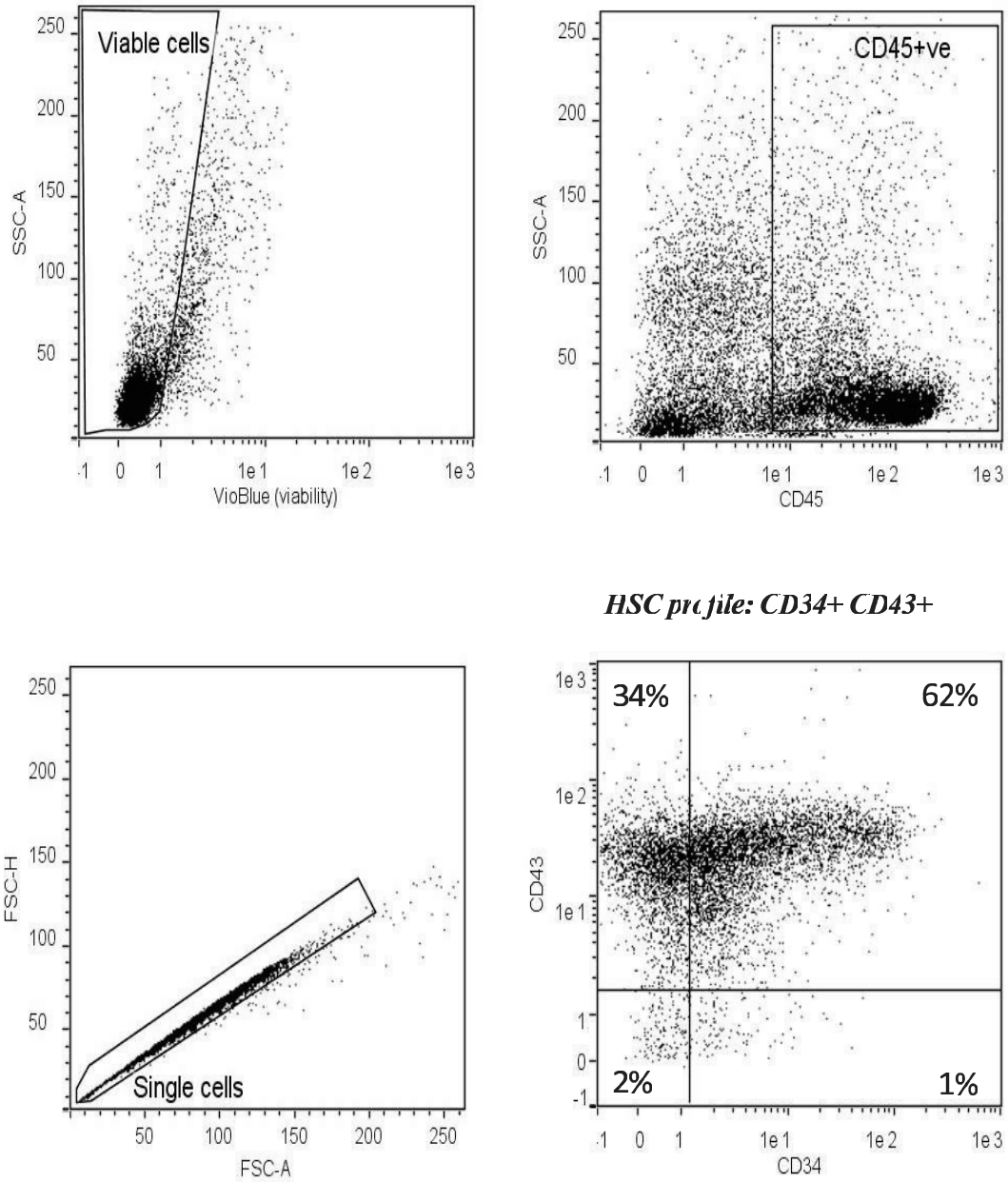


Figure 7
T cells are present after 9 days culture on OPDL-1 cells

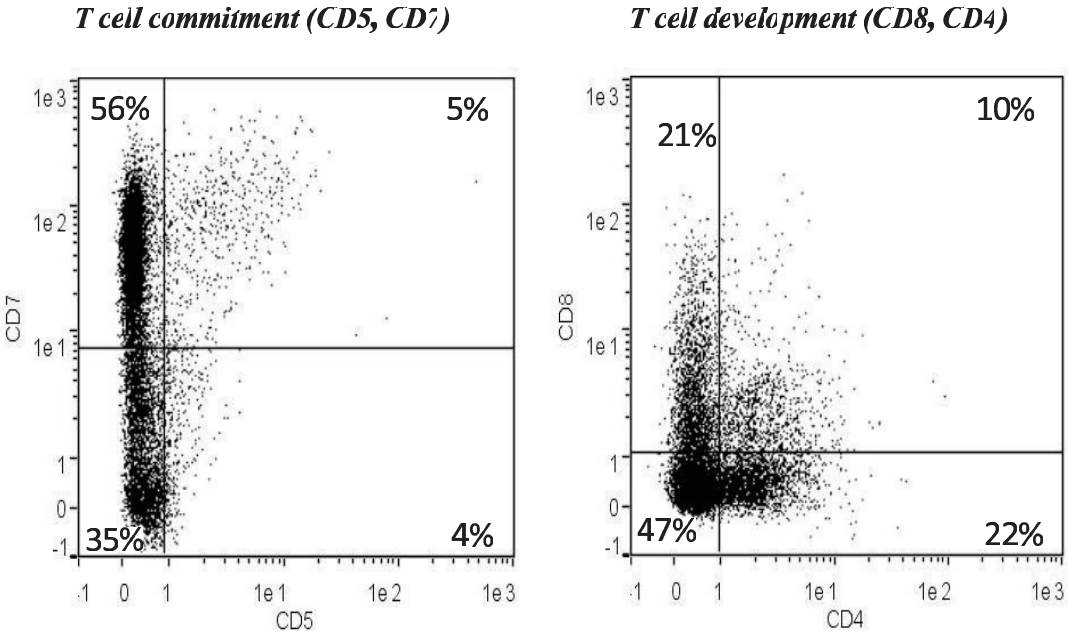


Figure 8
Mature (CD3+α/β TCR+) CD8+ T cells are present after 16 days in culture on OPDL-1 cells

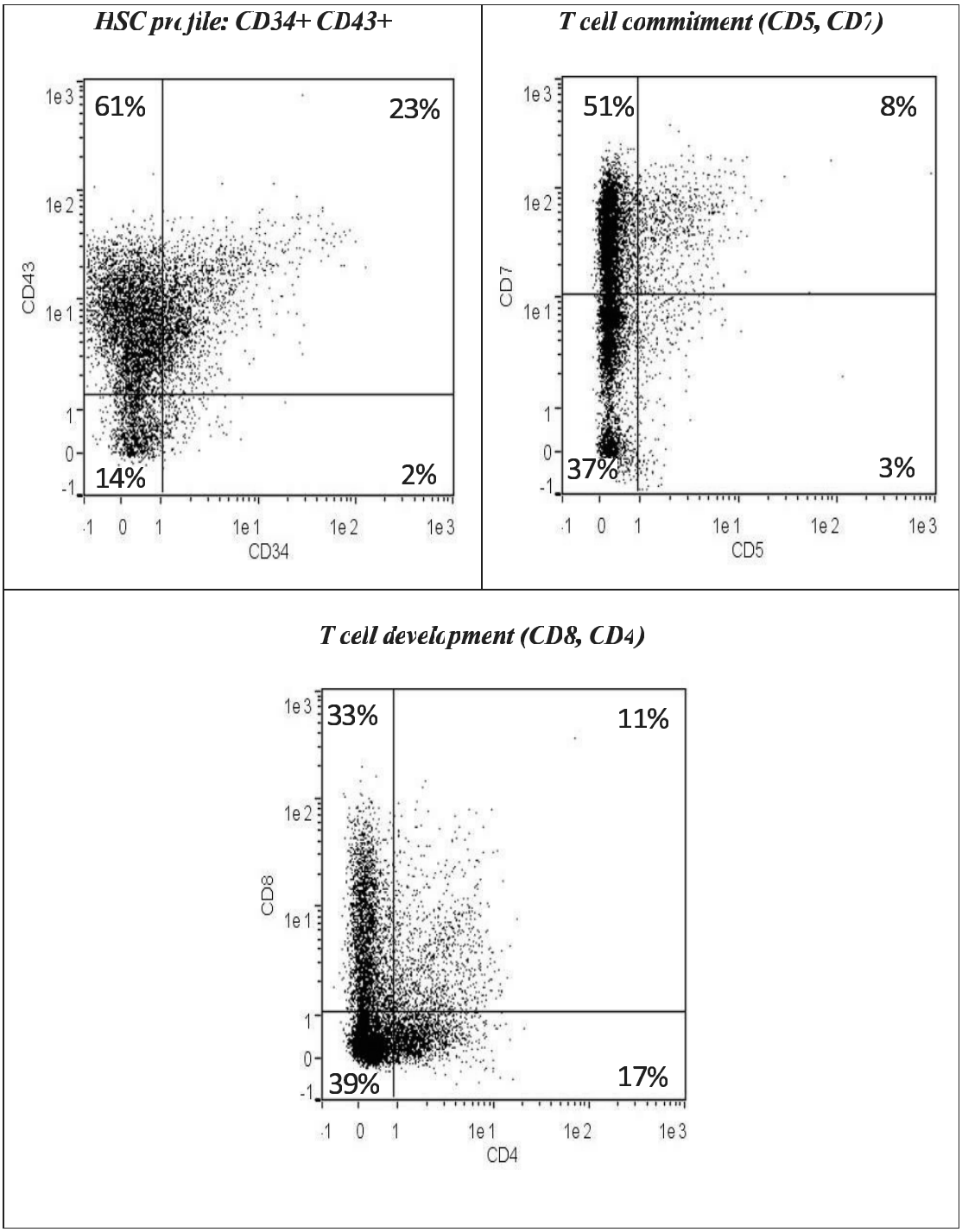


Figure 8 (Continued)

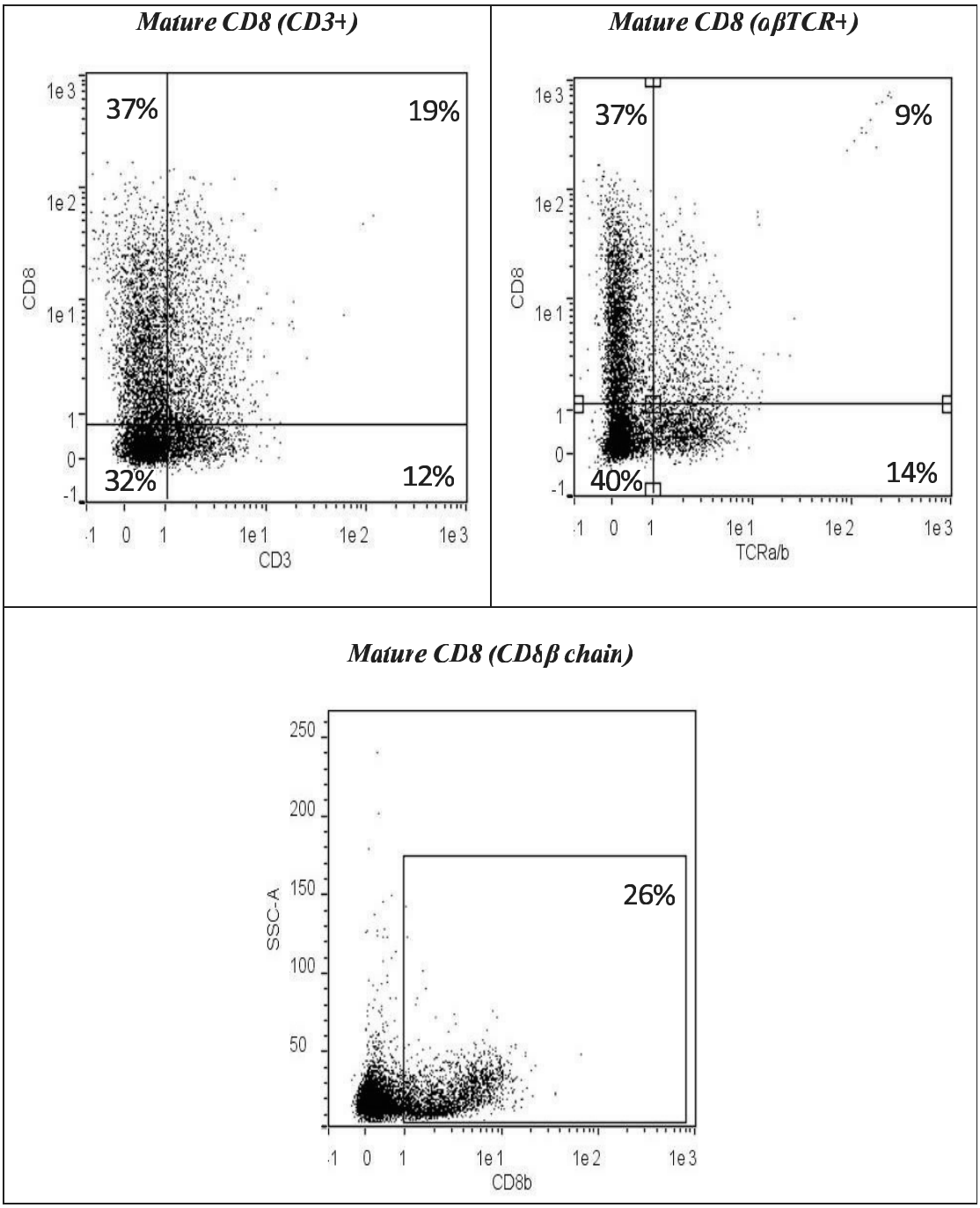


Figure 9
Schematic representation of the induction of WT-1 specific TCR, CD8αβ T cells from iPSC

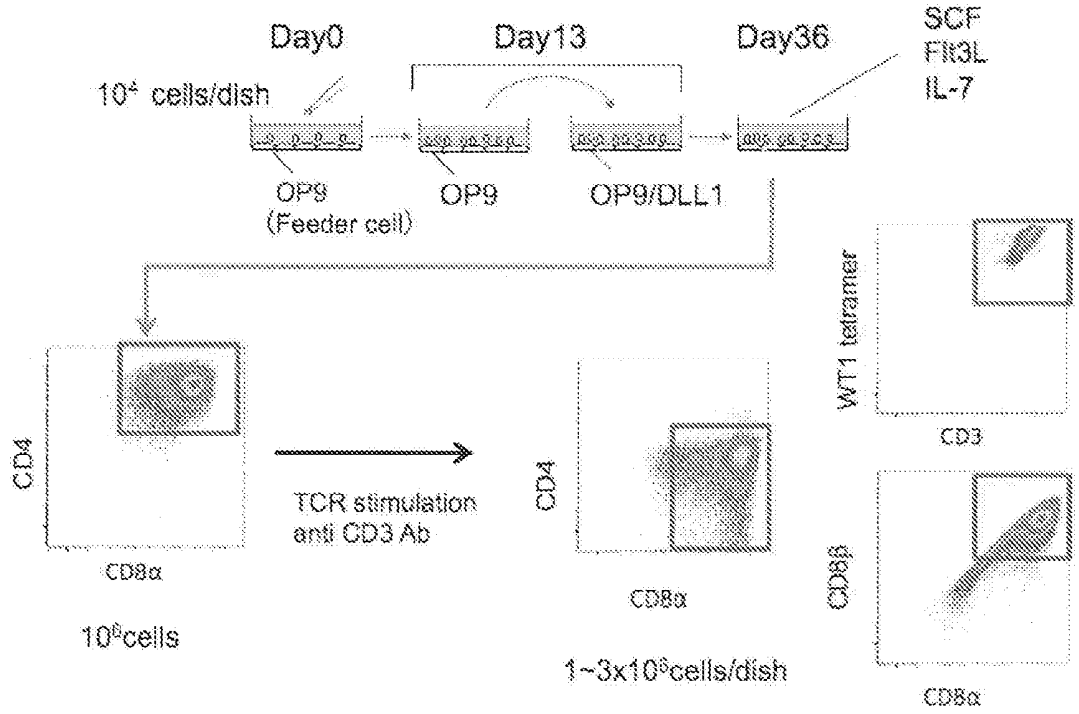


Figure 10
Function of WT-1 specific TCR, CD8αβ T cells induced from iPSC

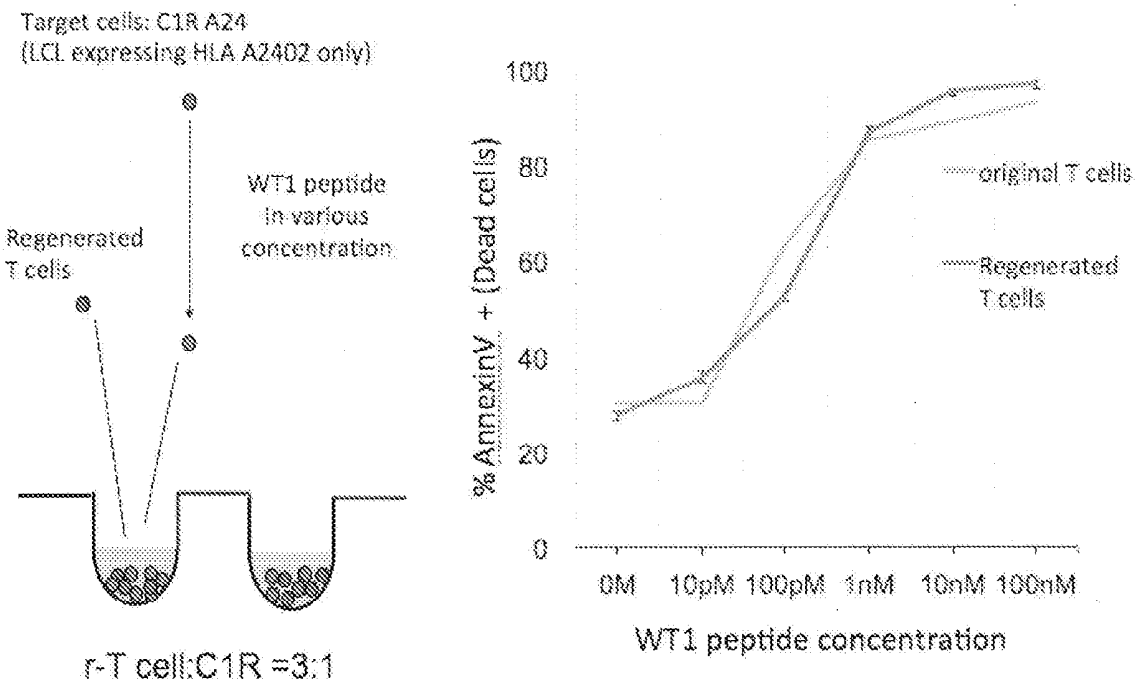


Figure 11

Schematic diagram of chimeric antigen receptor and antigen-binding receptor constructs

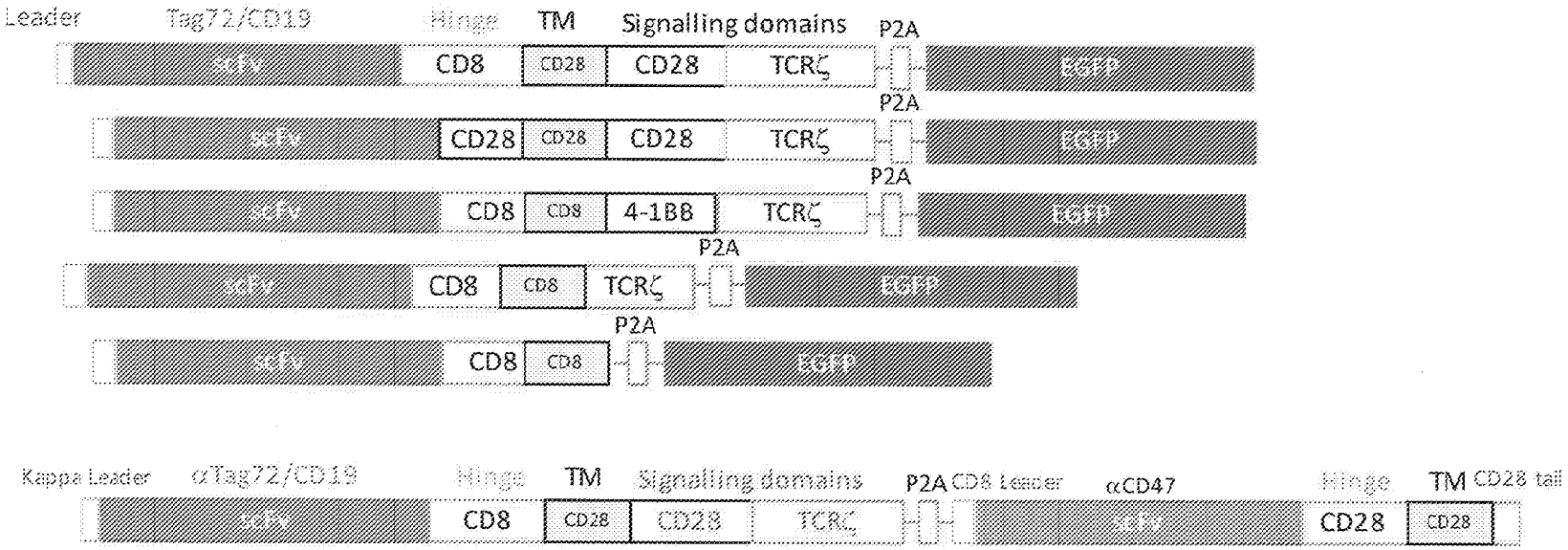


Figure 12
Retrovirus Transformation scheme

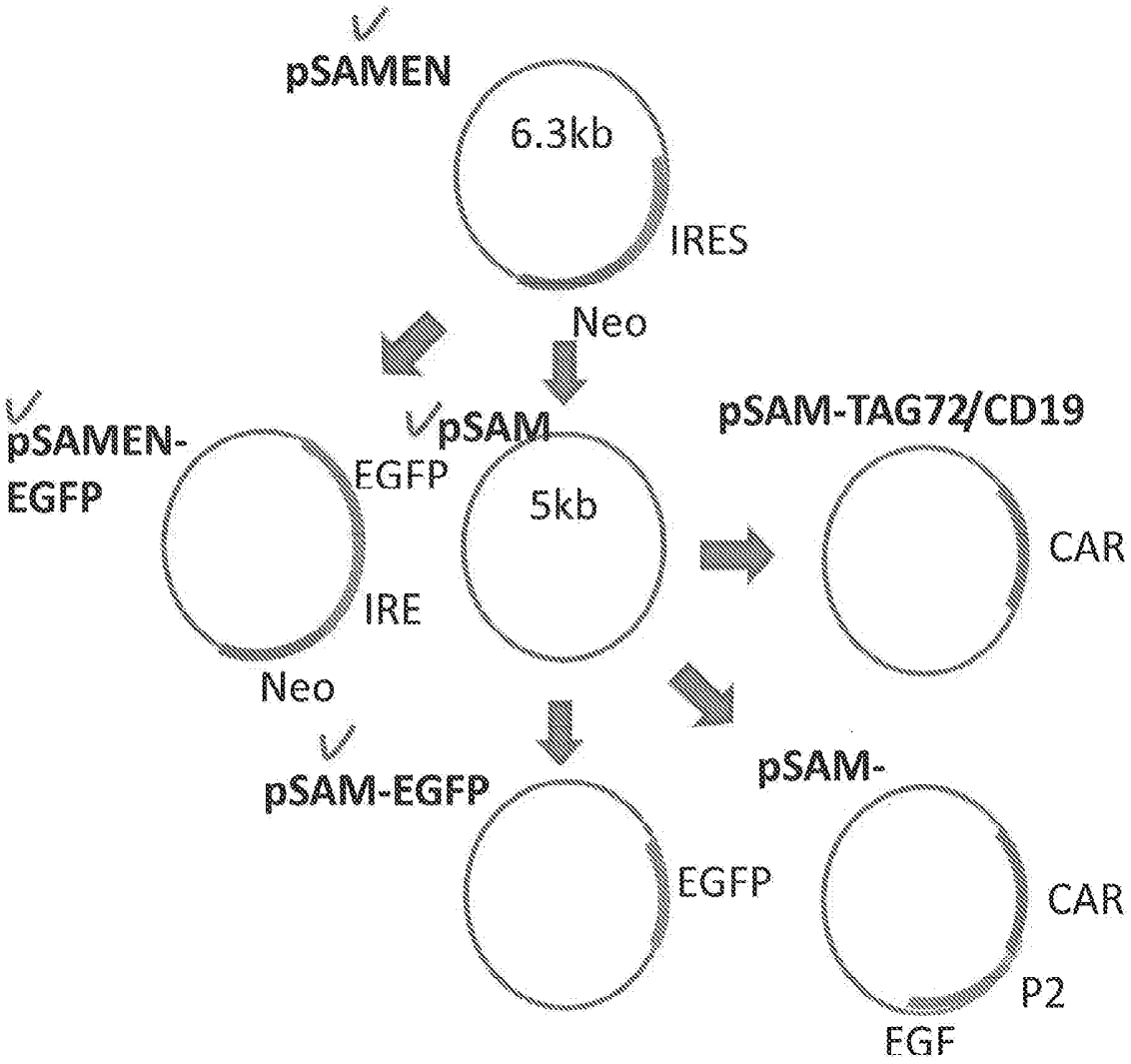
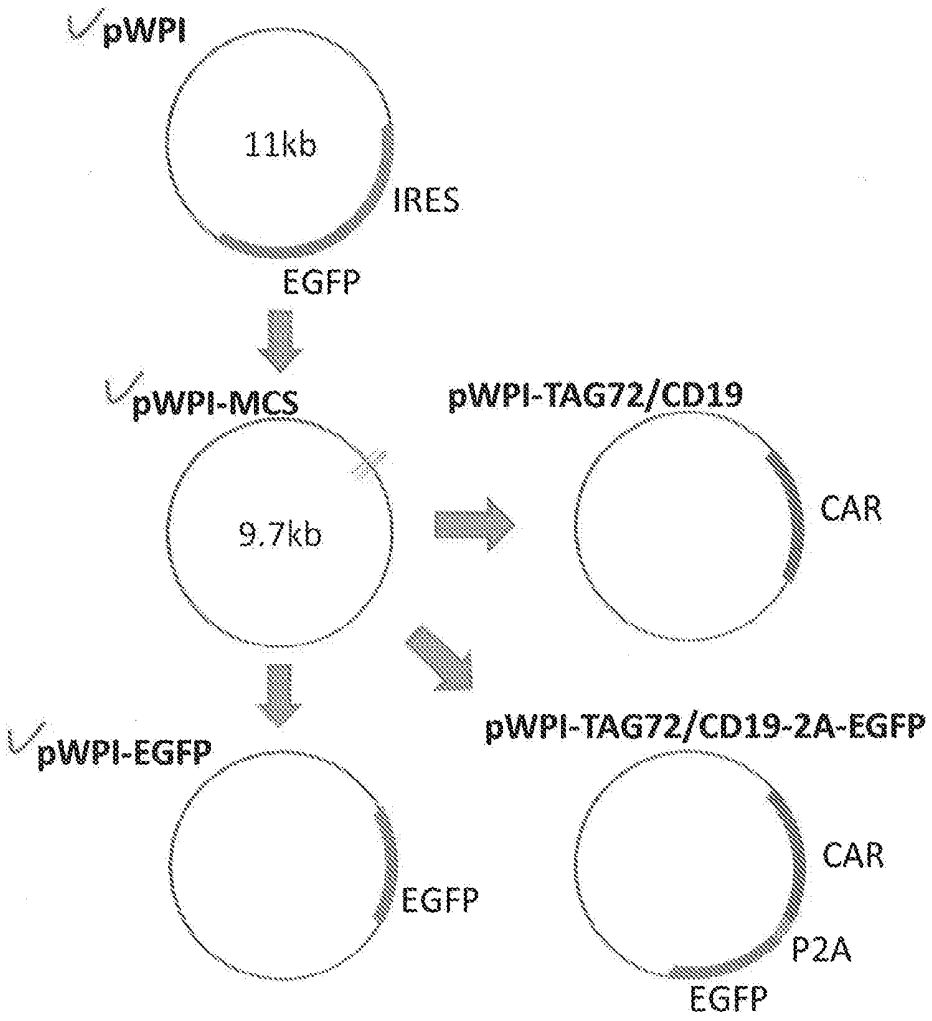


Figure 13
Lentivirus Transformation scheme



Figures 14A-14B
Schematic of a non-signalling antigen-binding receptor, a truncated CD47 "attachment stalk"

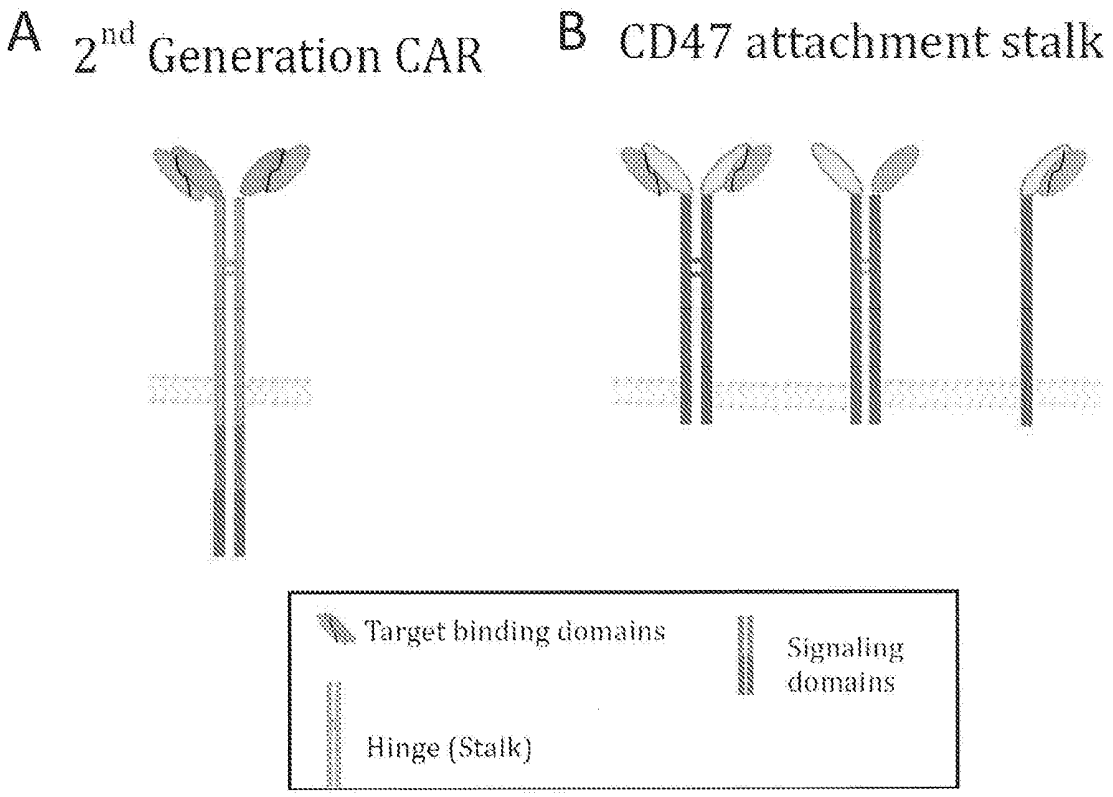


Figure 15
Flow cytometry analysis of CAR-transduced human PBMC-derived CD3+ T cells

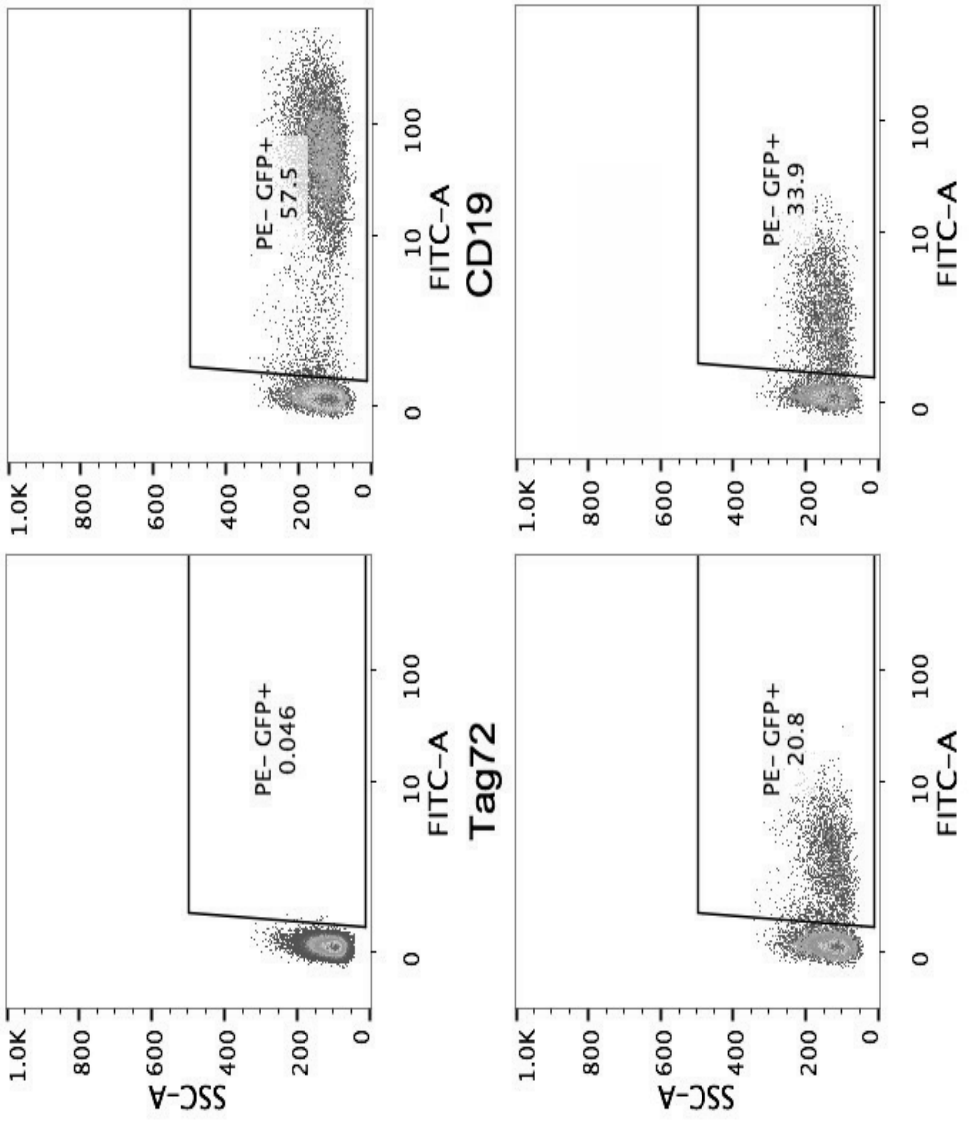
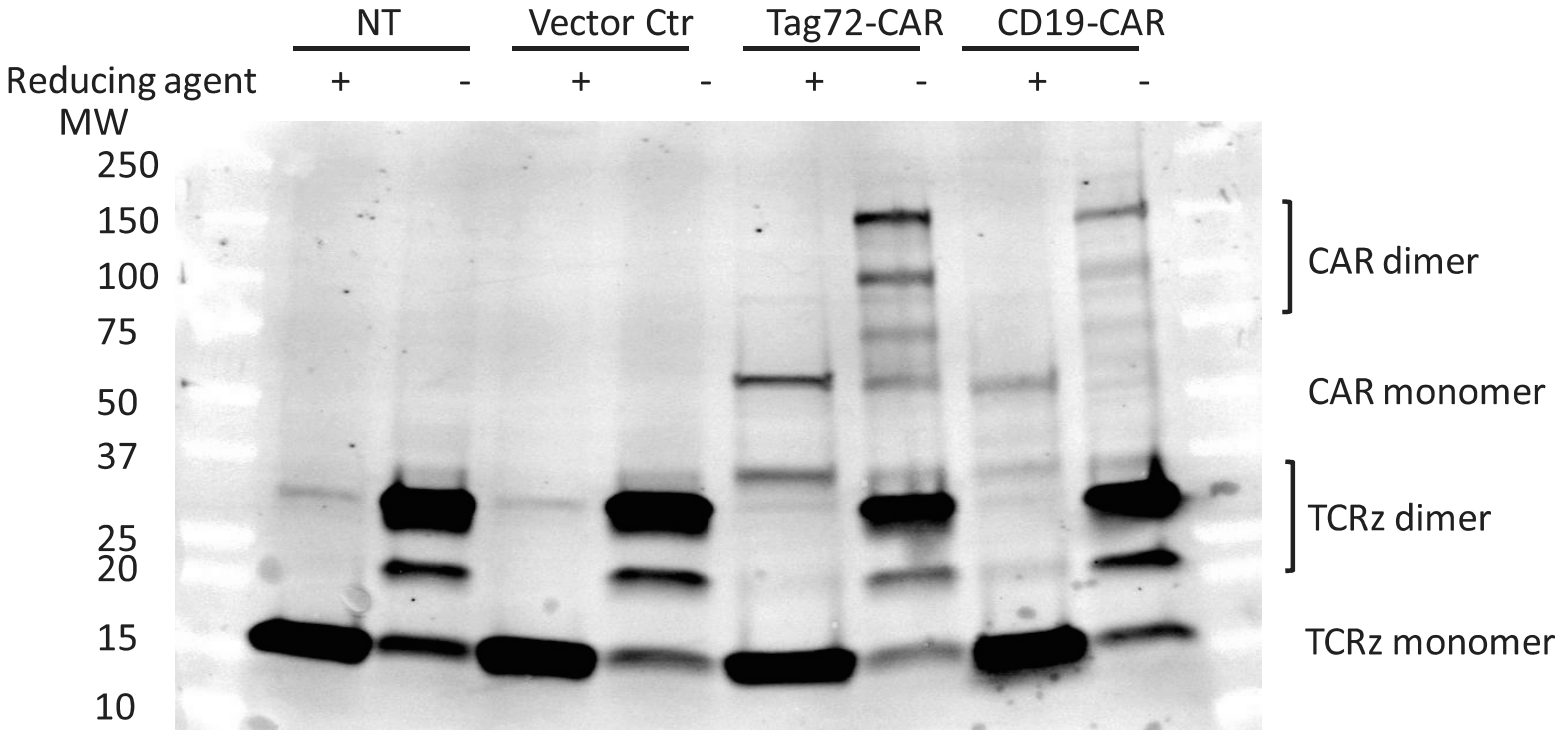


Figure 16

Western blot analysis confirming protein expression in TAG72 and CD19 CAR-transfected T cells



Western blot analysis of Tag72-CAR and CD19-CAR transduced human T cells under reducing (+) and non-reducing condition (-). It shows that the CARs are present as both covalent dimers and monomers within T cells.

Figure 17
TAG-72 CAR-T mediated killing of ovarian cancer cell line

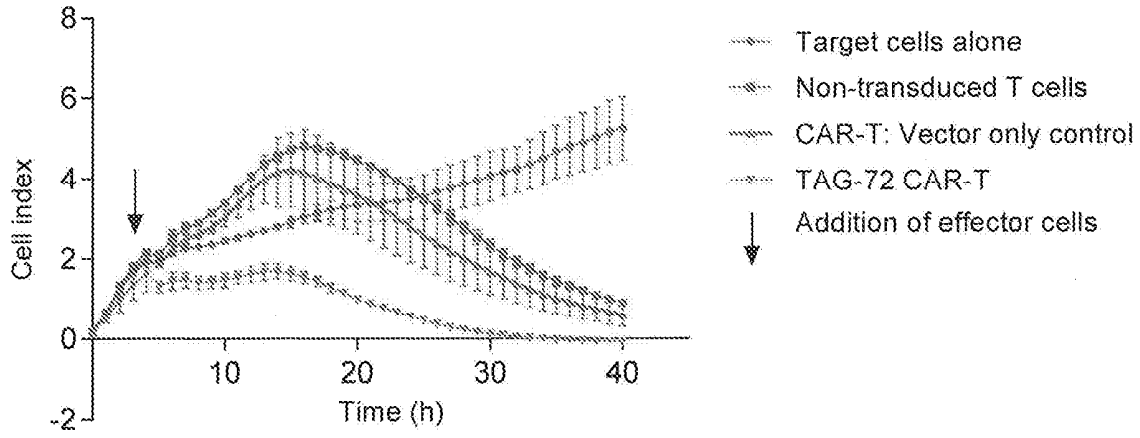


Figure 18
Specificity of TAG-72 CAR-T killing

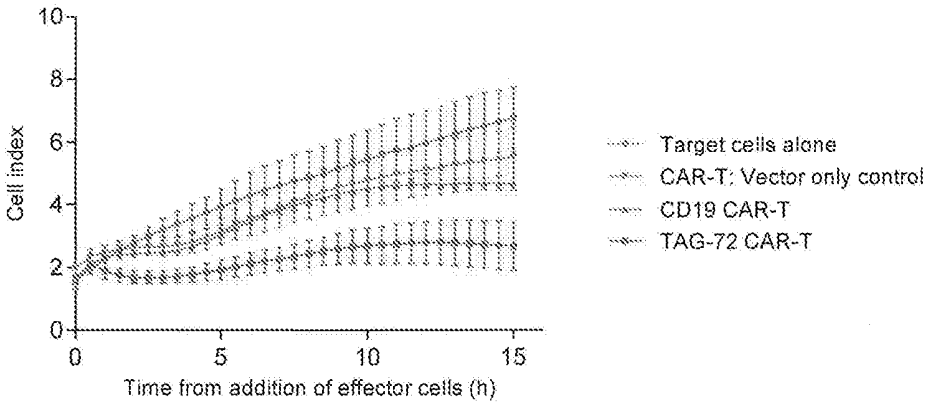


Figure 19A

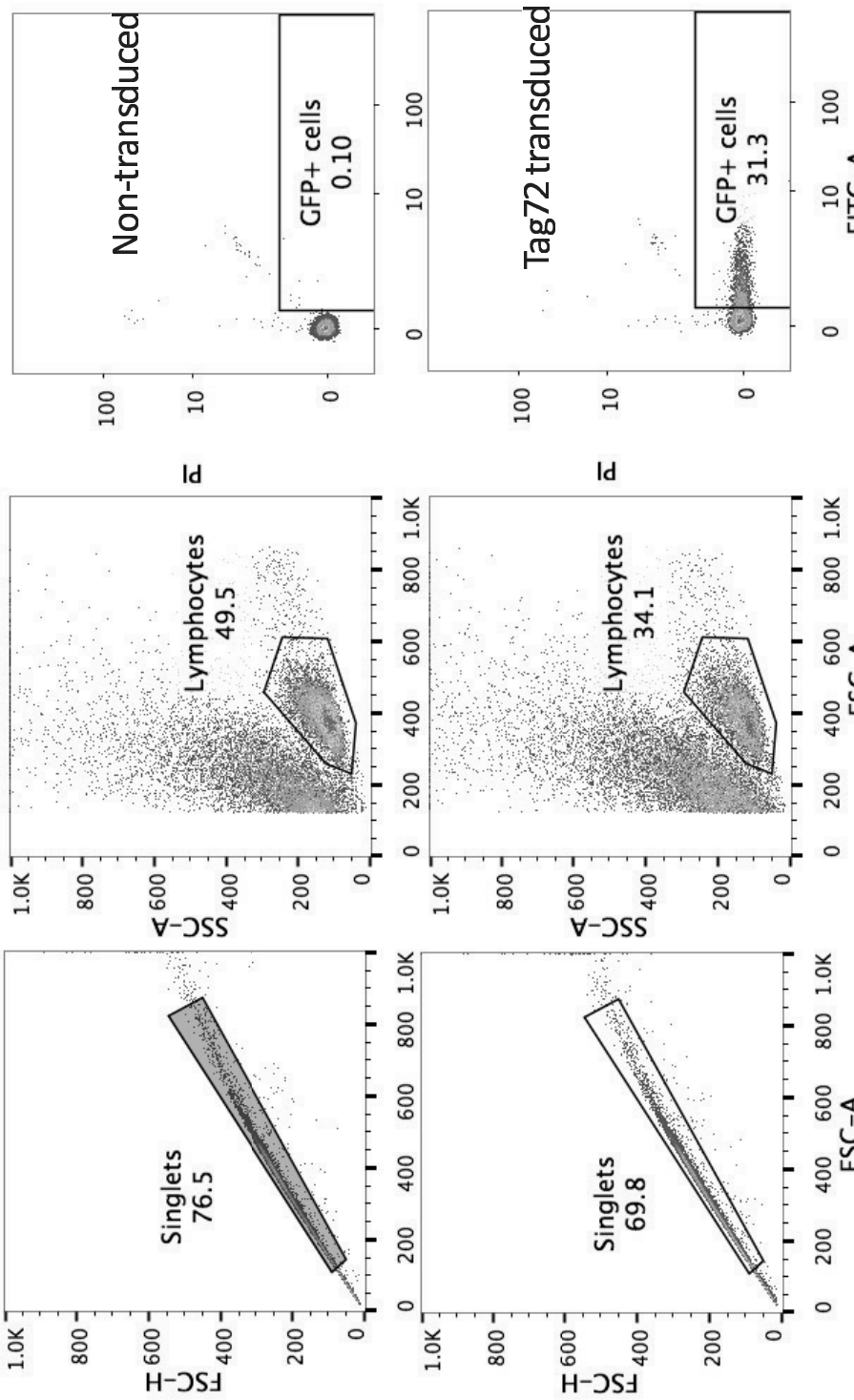


Figure 19A: Successful transduction of WT-1 specific TCR cytotoxic T cells derived from iPSCs produced from WT-1 specific TCR, with a CAR construct encoding TAG72

Figure 19B

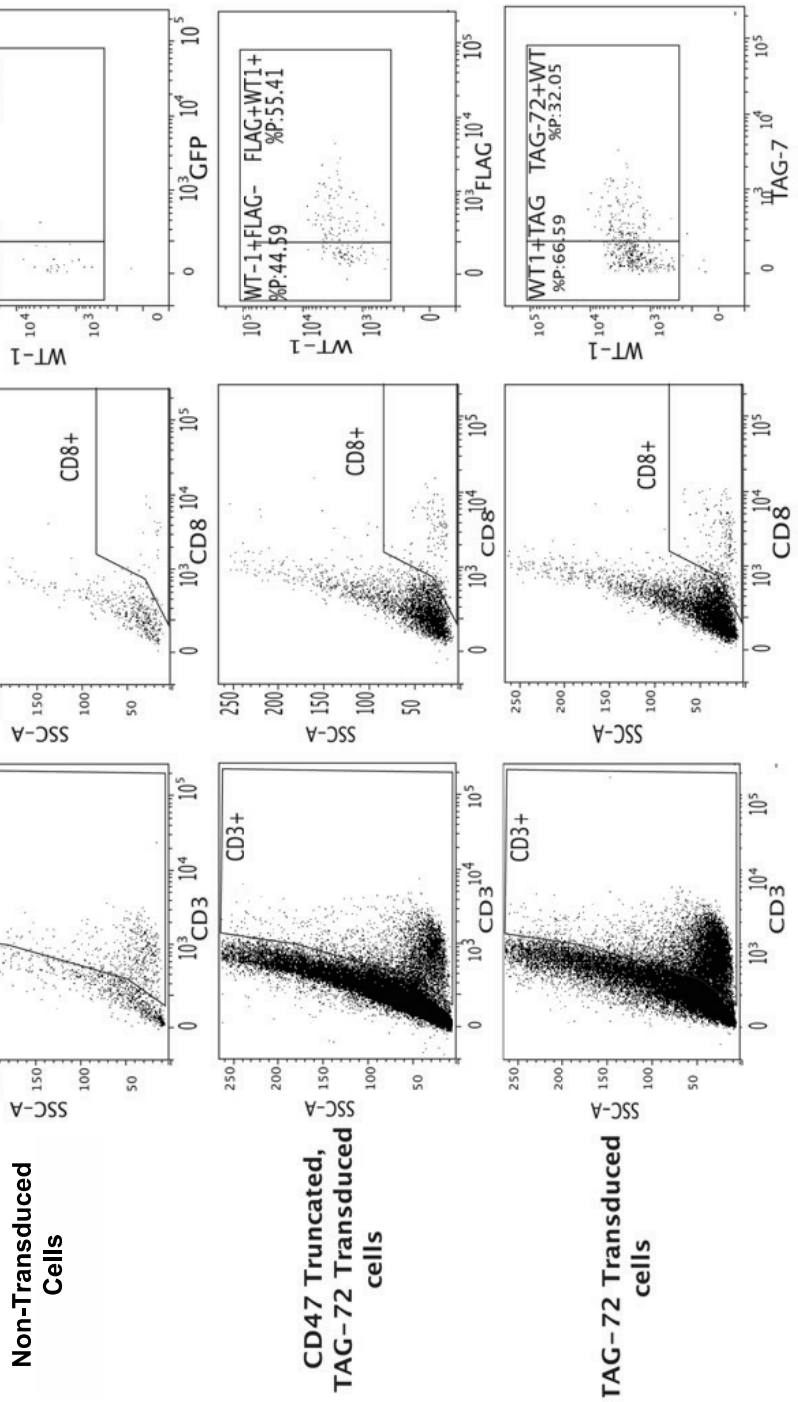


Figure 19B. Successful transduction of WT-1 specific TCR cytotoxic T cells derived from iPSC produced from WT-1 specific TCR T cells, with a CAR construct encoding TAG72 and truncated (non-signalling) CD47, as well as a TAG72 alone viral vector. Values are expressed as a percentage of CD8+ T cells.

Figures 20A-20I

Cytotoxicity of WT-1 TCR T cells, and dual specific TAG-72 CAR/WT-1 TCR T cells

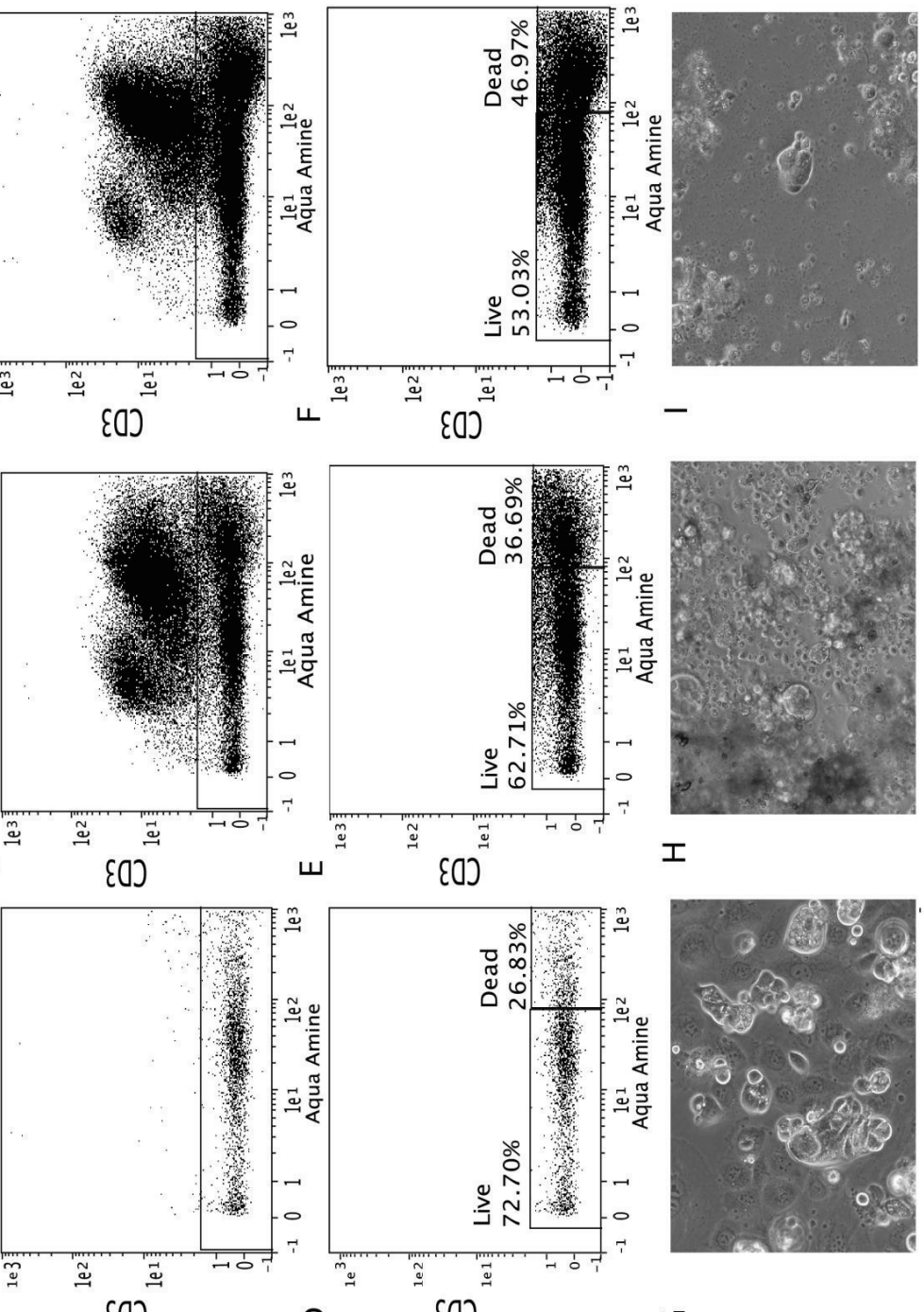


Figure 21A

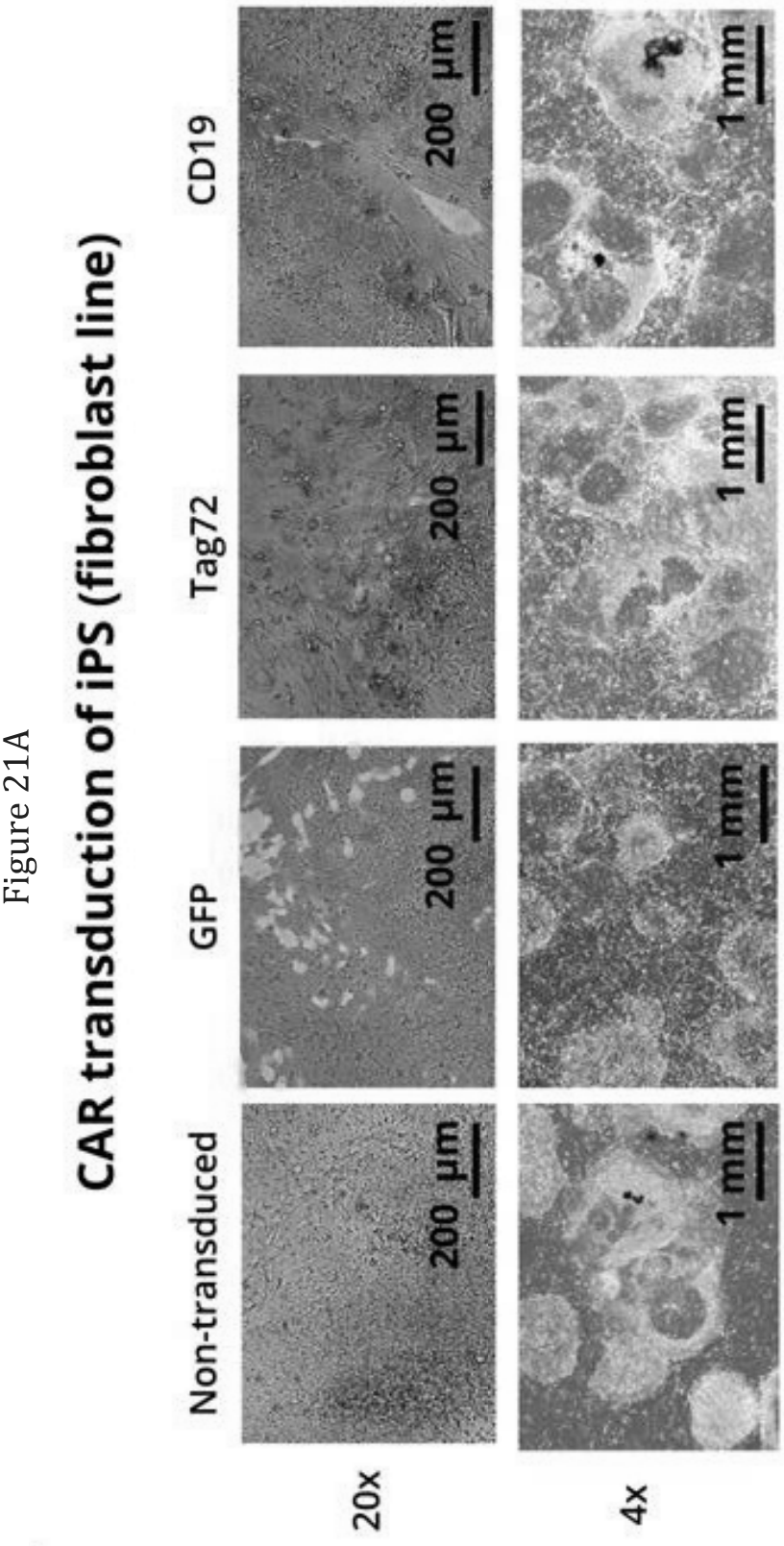

CAR transduction of iPS (fibroblast line)
Non-transduced
GFP
Tag72
CD19
20x
4x
200 µm
1 mm

Figure 21B
TAG 72 CAR transduction of iPSC derived from WT-1 Tcells

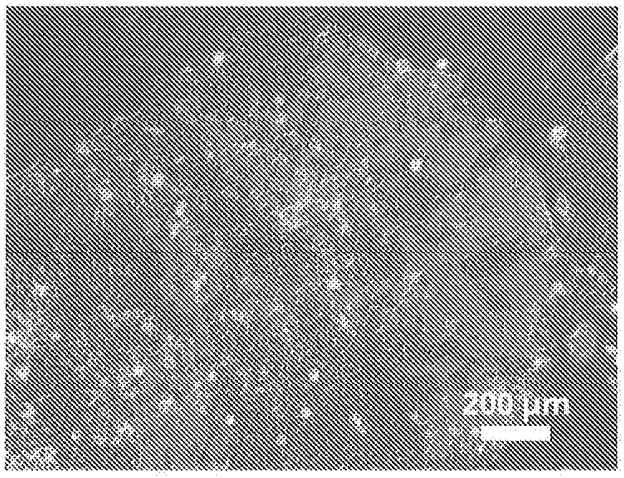


Figure 22

Flow cytometric analysis of Chimeric Antigen Receptor transduced iPSC

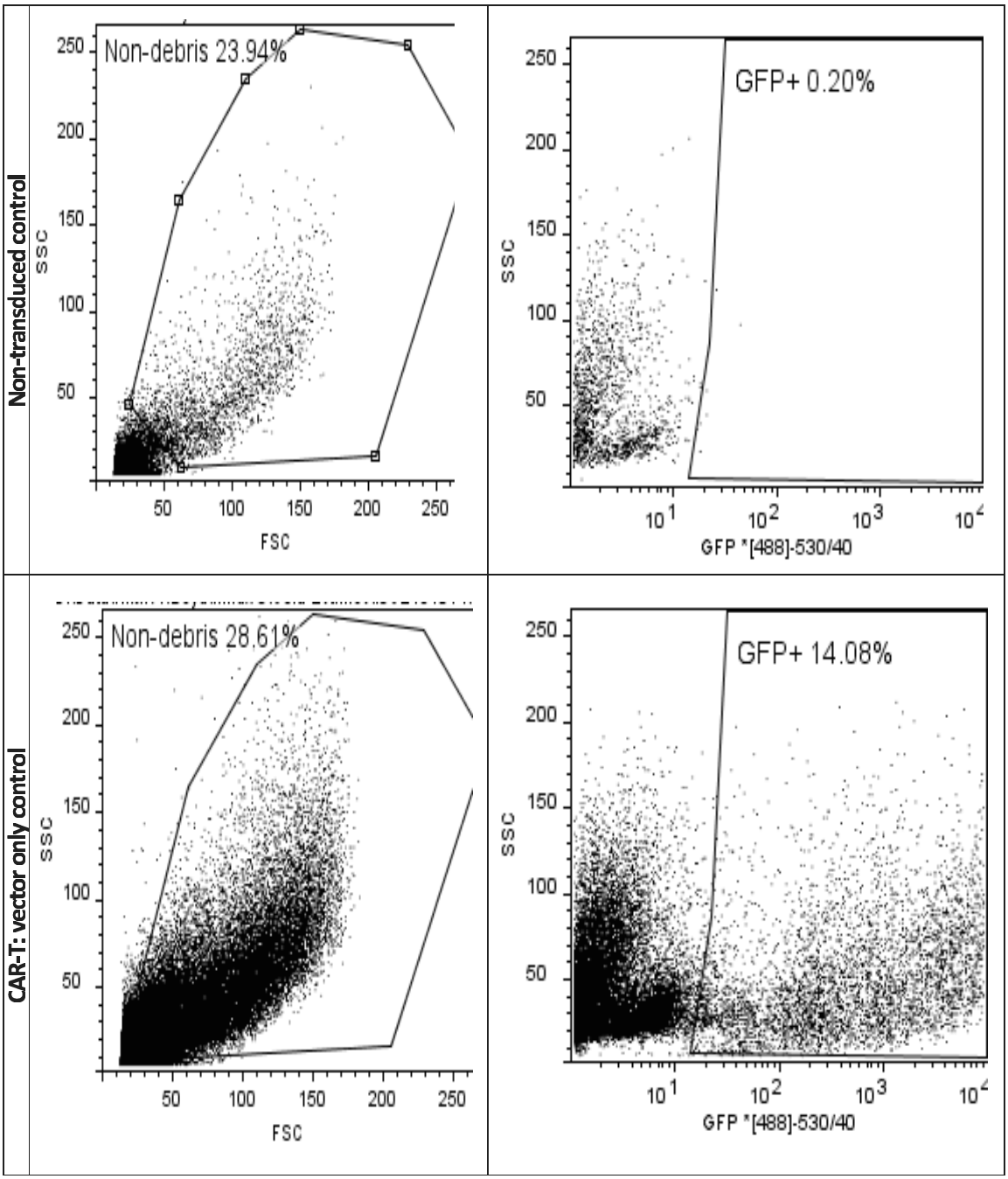


Figure 22 (Continued)

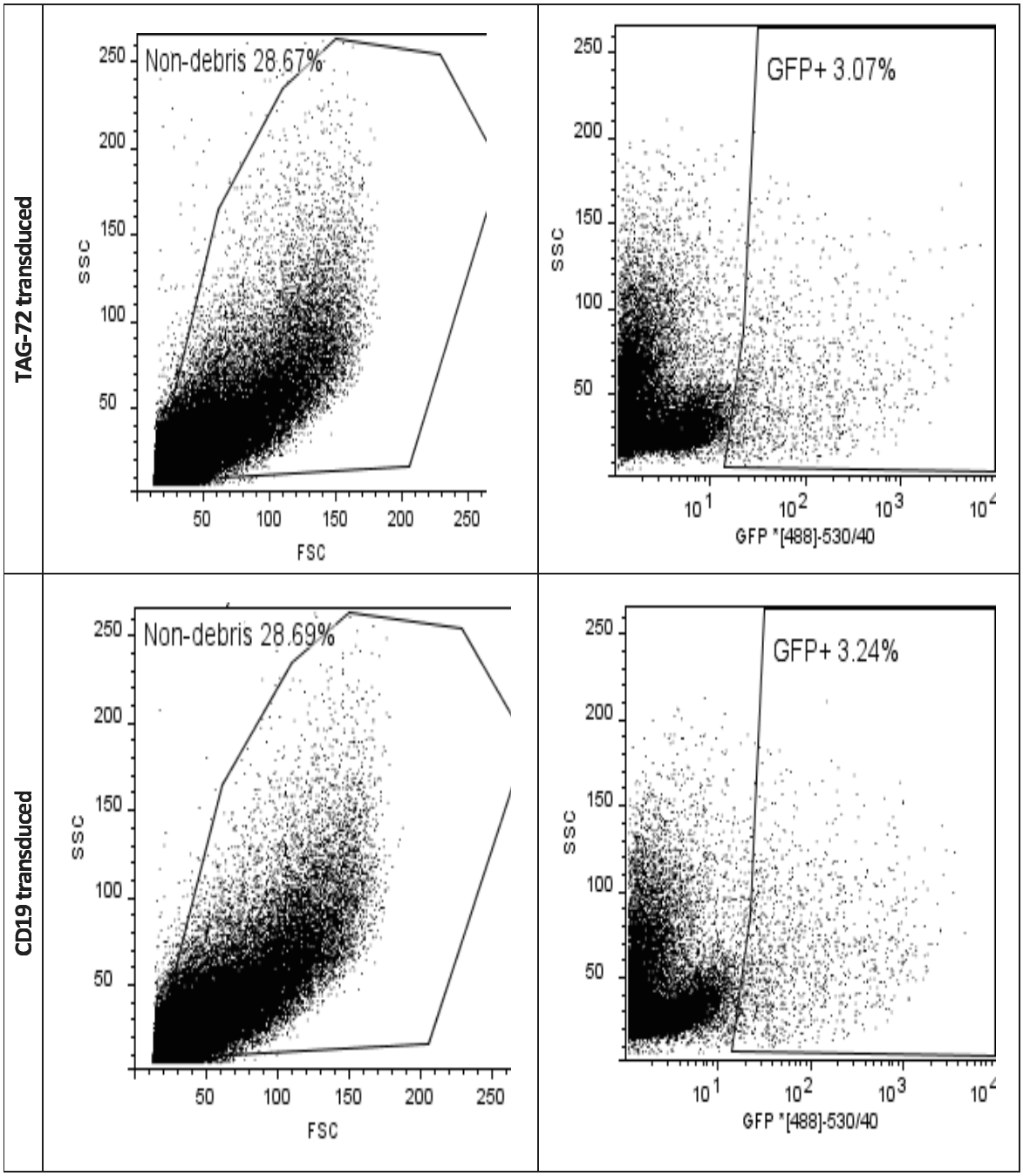


Figure 23

Overlay of dot plots comparing non-transduced control cells (blue) to CAR transduced iPSC cultures (green)

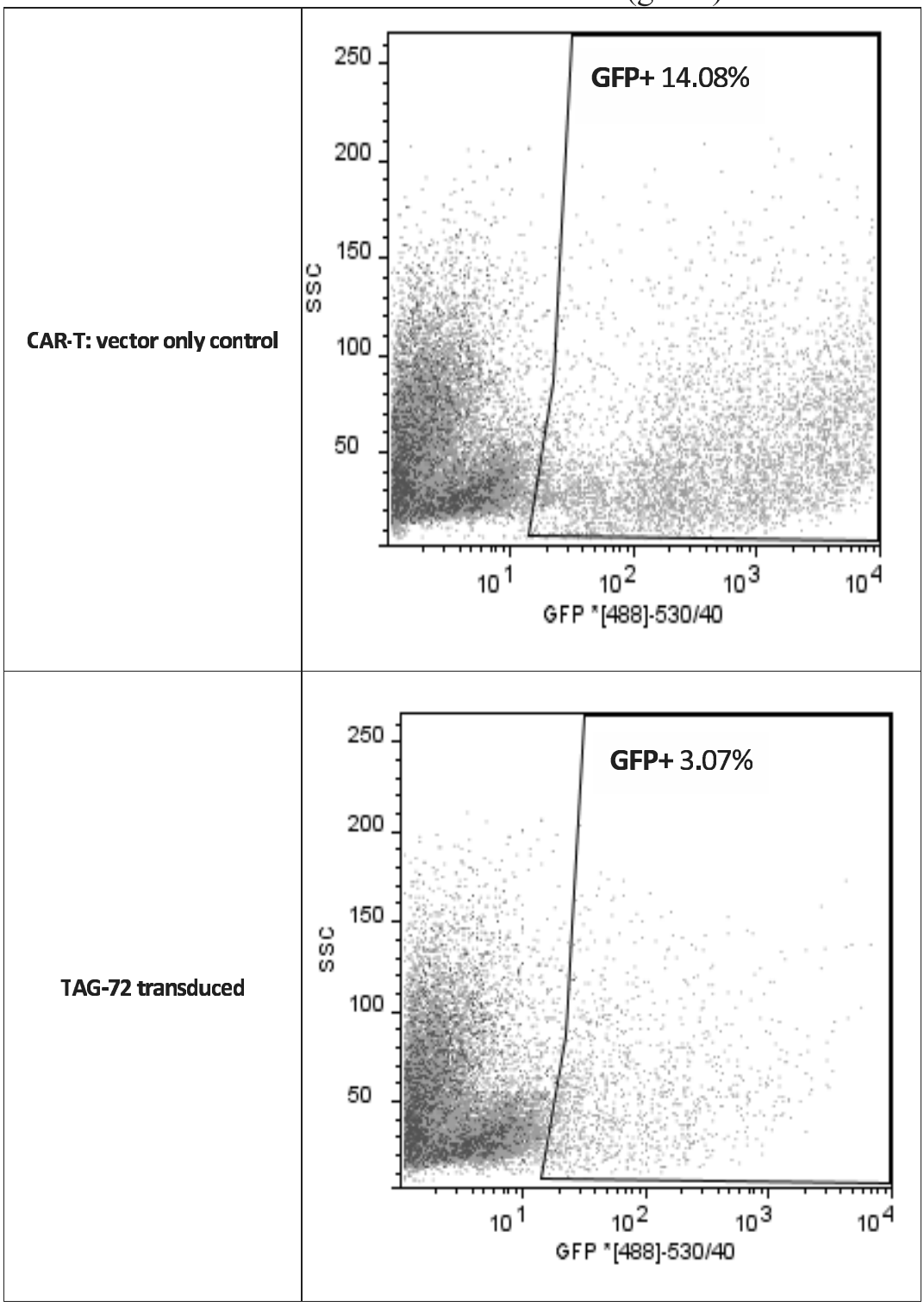


Figure 23 (Continued)

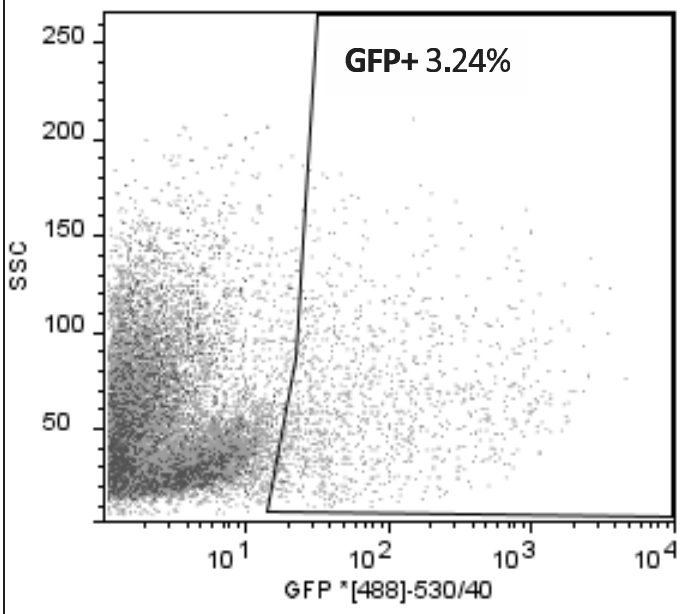
CD19 transduced	

Figure 24

Reformation of iPS colonies post sort on GFP+ FACS

